

AD 731702

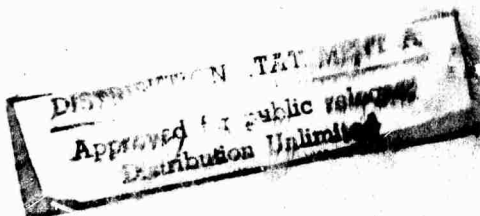


Reproduced by  
**NATIONAL TECHNICAL  
INFORMATION SERVICE**  
Springfield, Va. 22151



**AMERICAN OPTICAL  
CORPORATION**

CENTRAL RESEARCH LABORATORY • SOUTHBRIDGE, MASS. 01550



31

## DOCUMENT CONTROL DATA - R &amp; D

(Security classification of title, body of abstract and indexing annotation must be entered when the overall report is classified)

1. ORIGINATING ACTIVITY (Corporate author) American Optical Corporation Central Research Laboratory Southbridge, MA. 01550		2a. REPORT SECURITY CLASSIFICATION Unclassified	
		2b. GROUP N/A	
3. REPORT TITLE  NEODYMIUM LASER GLASS IMPROVEMENT PROGRAM			
4. DESCRIPTIVE NOTES (Type of report and inclusive dates) Technical Summary Report 1 July 1967 - 31 December 1967			
5. AUTHOR(S) (First name, middle initial, last name)  Richard F. Woodcock			
6. REPORT DATE July 1971		7a. TOTAL NO. OF PAGES 27	7b. NO. OF REFS 0
8a. CONTRACT OR GRANT NO. Nonr 3835(00)		8a. ORIGINATOR'S REPORT NUMBER(S) TR-598-11	
b. PROJECT NO. 7300			
c. ARPA ORDER 306		8b. OTHER REPORT NO(S) (Any other numbers that may be assigned this report)	
d.			
10. DISTRIBUTION STATEMENT  Distribution of this report is unlimited			
11. SUPPLEMENTARY NOTES  Project DEFENDER		12. SPONSORING MILITARY ACTIVITY  Office of Naval Research Washington, D.C.	
13. ABSTRACT  This report continues detailing efforts expended toward achieving a means for measuring the stress optical coefficients of laser glass test specimens using a 3-pinhole interferometer. The apparatus design and construction is discussed. The experimental procedure is delineated and some initial results are presented. Finally a theoretical analysis of tolerance studies of the interferometer is appended.			

14. KEY WORDS	LINK A		LINK B		LINK C	
	ROLE	WT	ROLE	WT	ROLE	WT
LASERS LASER GLASS INTERFEROMETER						

This research is part of Project DEFENDER under the joint sponsorship of the Advanced Research Projects Agency, the Office of Naval Research and the Department of Defense.

Reproduction in whole or in part is permitted by the United States Government.

Distribution of this document is unlimited.

NEODYMIUM LASER GLASS  
IMPROVEMENT PROGRAM

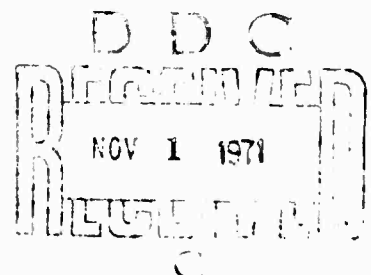
Technical Summary Report

Number 11  
July 1971

Dr. Richard F. Woodcock

Contract No. Nonr-3835(00)  
Project Code No. 7300  
ARPA Order No. 306

American Optical Corporation  
Central Research Laboratory  
Southbridge, Mass. 01550



## ABSTRACT

This report continues detailing efforts expended toward achieving a means for measuring the stress optical coefficients of laser glass test specimens using a 3-pinhole interferometer. The apparatus design and construction is discussed. The experimental procedure is delineated and some initial results are presented. Finally a theoretical analysis of tolerance studies of the interferometer is appended.

## FOREWORD

This report has been prepared by the Central Research Laboratory of the American Optical Corporation, Southbridge, Massachusetts under Contract Nonr 3835(00) entitled "Neodymium Laser Glass Improvement Program." The contract is under the sponsorship of the Office of Naval Research and this report covers the six-month period ending 31 December 1967.

Dr. Richard F. Woodcock is project manager. Luther Smith was involved in the design, analysis and operation of the pinhole interferometer described herein. Theoretical considerations included as Appendix I were carried out by Dr. H. Osterberg and L. Smith.

This program is part of project DEFENDER.

This report is unclassified.

## CONTENTS

	PAGE
1. INTRODUCTION AND SUMMARY. . . . .	1
2. APPARATUS DESIGN. . . . .	2
2.1 AUTOCOLLIMATOR AND PINHOLE ASSEMBLY. . . . .	4
2.2 METHOD OF POLARIZATION . . . . .	5
2.3 UNIFORMITY OF STRESS IN THE GLASS SPECIMEN . . . . .	6
2.4 PRECISION STRAIN FRAME . . . . .	7
3. EXPERIMENTAL PROCEDURE. . . . .	10
APPENDIX: TOLERANCE STUDIES ON THE INTERFEROMETER . . . . .	13

## ILLUSTRATIONS

	PAGE
Figure 1. Diagram of the three-pinhole interferometer for measuring the stress-optical effect in glass samples. . . . .	3
Figure 2. Autocollimator and pinhole subassembly. . . . .	4
Figure 3. Photograph of the strain frame. . . . .	8
Figure 4. Schematic drawing of the strain frame . . . . .	9
Figure 5. Experimental setup used for complete measurement of stress induced pathlength changes . . . . .	10



## NEODYMIUM LASER GLASS IMPROVEMENT PROGRAM

### 1. INTRODUCTION AND SUMMARY

This technical summary covers work performed under contract NONR 3835 (00) during the six-month period ending 31 December 1967. Efforts during this period have been concerned primarily with the construction and testing of a three beam interferometer for the measurement of stress optical coefficients.

The design and fabrication of subassemblies completed during this period for the interferometer previously described (NONR-3835 (00) Technical Summary Report #10 March 1971) include an autocollimating device for aligning the light source of the interferometer, an accurate lever type strain frame for applying stress to the sample, and a half wave plate for rotating the plane of polarization of light from the laser source plus a rotatable linear polarizer on the eye piece of the microscope. The latter were added for greater convenience and reliability in making the measurements to obtain the separate stress optical coefficients for light vibrating parallel to the direction of stress and for light vibrating perpendicular thereto. The final design of the subassemblies and their necessity were determined in part by an investigation, both theoretical and experimental, of permissible tolerances in various components of the interferometer.

This investigation indicates that the apparatus can measure pathlength changes induced by stress in the glass samples to an accuracy of  $\lambda/100$ ,  $\lambda=6328$  Angstroms, but that nonuniformity of stress within the test specimen may limit the accuracy of the determination to somewhat less than this. A detailed treatment of these tolerance studies is given in the appendix.

Assembly of the interferometer is complete and it has been tested by making duplicate measurements on a test sample to check reproducibility of results. These measurements yielded pathlength changes that vary from one set of measurements to the next by up to about 0.05 wavelengths. This variation represents an inaccuracy in the determination of induced pathlength change of no more than 3%. It should be possible to determine the stress optical coefficients by this method and apparatus to  $\pm 10\%$  assuming that correct values for Young's Modulus and Poisson's Ratio can be obtained for the glass samples. A description of the completed system and the procedure for its use is included.

Melting of athermal glass compositions with improved optical quality has continued during this period and test specimens have been fabricated from selected portions of these melts for the determination of Young's Modulus, Poisson's Ratio and the change in optical thickness as a function of pressure and plane of polarization.

The present contract was scheduled to terminate July 21, 1967. In view of a several month delay between the effective starting date and notification of award of the contract and of the status of the work a request was made in June of 1967 to extend the termination date to March 31, 1968. This request has now been granted. Measurement of the stress optical coefficients of the above athermal glass composition will be carried out during the remainder of the contract.

## 2. APPARATUS DESIGN

Investigation of the tolerances of various components of the apparatus for measuring stress optical coefficients has continued. Results of these studies have helped in the design of the apparatus and procedures for its use in measuring the stress optical properties of glass samples which contain some optical stria. The final design for the system is shown in Figure 1.

The study on component tolerances indicates that; (1) defocusing of the collimator in the arrangement of Figure 1 by relatively slight amounts will not alter the accuracy of the measurement of the induced change in pathlength (Appendix I.1), (2) the tolerances on the setting of the polarizer or analyzer, using either the "X-Y Method" or the "45° Method" are large enough so that no difficulty need be expected, (Appendix I.2 and I.3) (3) the presence of wedge in the test specimen does not affect the measurement of the change in optical pathlength as a function of applied pressure but in order that the light diffracted from the three pin holes shall overlap properly in the plane of observation, the degree of wedge in the sample should not exceed about 2.7 minutes, (Appendix I.5, I.6 and I.8) (4) surface flatness does not affect optical pathlength measurements, (Appendix I.7) and (5) the plane of the front surface of the sample should be normal to the incident light beam within approximately 7 minutes (Appendix I.9).

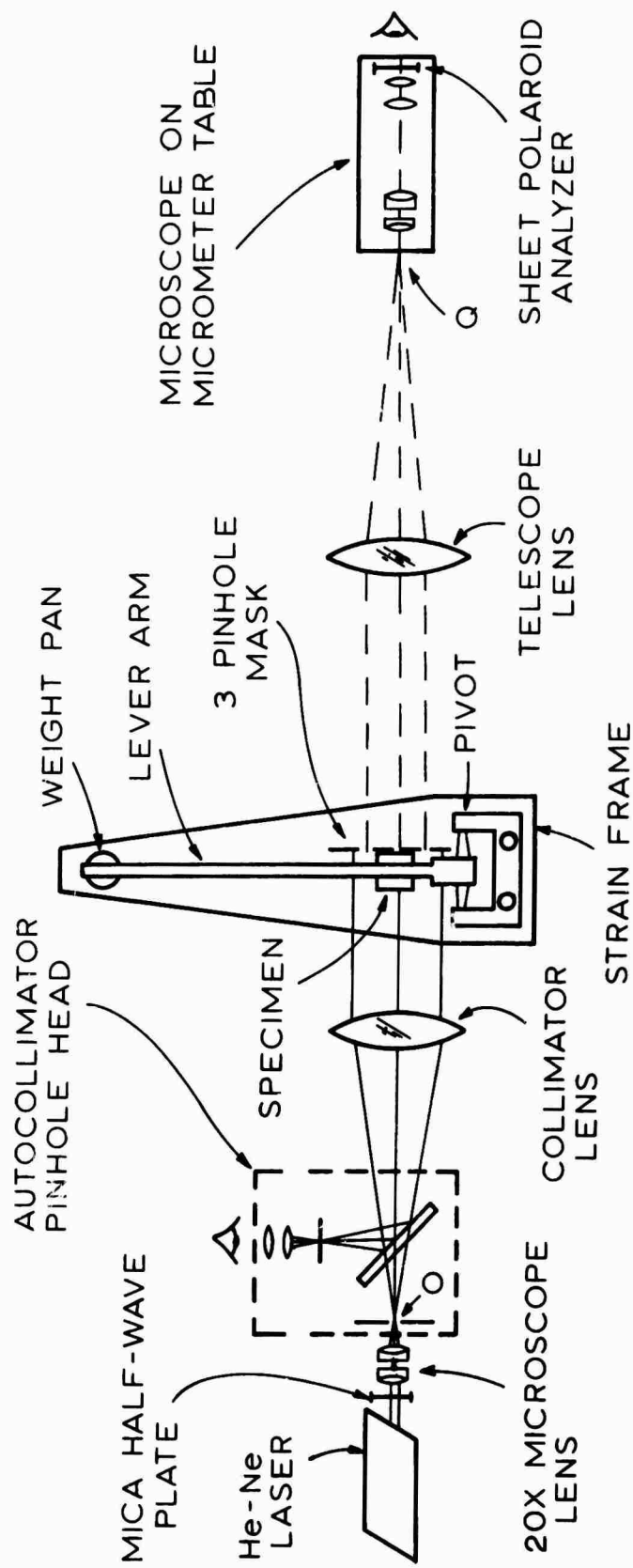


Figure 1. Diagram of the three-pinhole interferometer for measuring the stress-optical effect in glass samples.

## 2.1 AUTOCOLLIMATOR AND PINHOLE SUBASSEMBLY

The need for some form of autocollimating device to monitor the alignment of the sample was indicated in the previous report (Technical Summary Report No. 10). The subassembly fabricated for this purpose is shown in Figure 2. With this device, setting the sample to within the allotted seven minute tolerance mentioned above should be an easy matter. This subassembly in addition

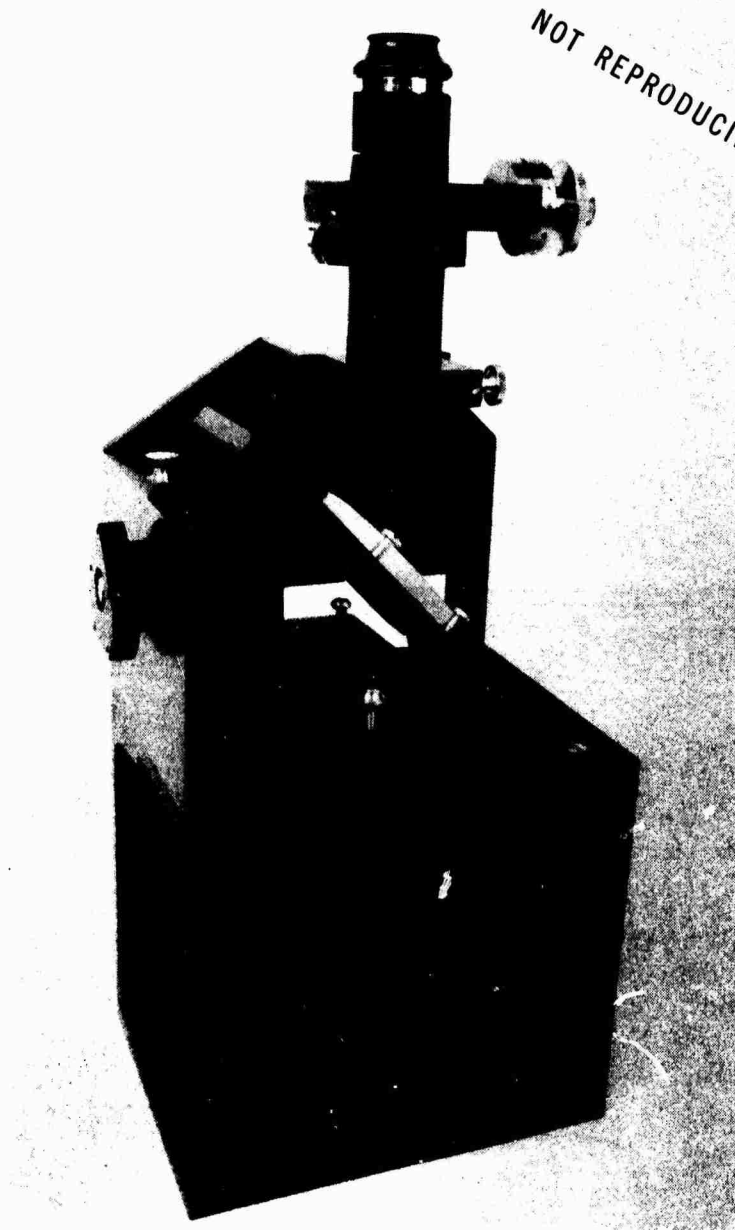


Figure 2. Autocollimator and pinhole subassembly.

contains the collimator pinhole (mounted on the left in Figure 2) with its own fine X-Y adjustment. The beamsplitter plate is adjustable with respect to both the base and the Filar Micrometer Eyepiece which serves as the eyepiece of the autocollimator.

## 2.2 METHOD OF POLARIZATION

The laser in Figure 1, in its normal position, emits an E-vector that vibrates approximately along Z, the line of the applied pressure. A rotatable half-wave plate was mounted external to the laser cavity in order to obtain other planes of vibration easily. Two methods of choosing the plane of polarization of the sampling beam were considered which are designated herein as the "X-Z Method" and the "45° Method." Tolerances on the angles of orientation involved in these two methods are such that either method should yield satisfactory results.

In the X-Z method the  $\lambda/2$ -plate is oriented so that the vector E is incident on the glass sample with E vibrating along Z or X. With moderate force on the sample, the glass becomes birefringent thus only light polarized parallel to the direction of stress (Z-axis) or normal to it will emerge plane polarized. Alignment of the incident E-vector along the Z or X axis may thus be accomplished with the aid of a crossed analyzer. By aligning the combination for minimum transmission these scale settings can be determined to about  $\pm 0.1^\circ$ .

The pathlength changes,  $\Delta\phi_Z$  and  $\Delta\phi_X$ , are observed by setting the  $\lambda/2$  plate so that the incident E-vector vibrates along Z and X respectively and measuring the change in interference pattern with stress. The advantages of this method are that little laser light is wasted and that no analyzer is needed in observing the fringe settings. The main disadvantage is that the  $\lambda/2$ -plate adjustment is out of reach of the operator while the fringes are being viewed.

In the 45° method the  $\lambda/2$  plate is set and left at a scale setting for which the incident E-vector at the strained glass sample vibrates near or at 45° with respect to Z and X. This setting is chosen to provide components of light in the Z and X directions of roughly equal intensities and need not be exact. The fringe patterns formed in the interferometer by each of these components coincide when the glass is stress-free, but as stress is applied they shift by different amounts and produce a composite pattern of generally reduced contrast. A linear polarizer over

the eyepiece of the microscope allows one to examine at will the fringe pattern from one of these components while eliminating the effect of the other simply by turning the polarizer to cross out the light of the unwanted direction of polarization.

In addition, the birefringence, which depends on the difference between the induced pathlength changes, can be measured directly by replacing the telescope lens with a Babinet-Soleil compensator followed by its own linear polarizer and adjusting it to remove and thus measure the relative phase difference between Z and X components of the light coming through the central pinhole and strained sample. This birefringence measurement is used as a cross-check on the measurements of the separate induced pathlength changes, since the difference calculated from the separate measurements made by using first the component vibrating in the Z direction, then that vibrating in the X direction should agree within experimental error with the difference measured directly using the compensator.

### 2.3 UNIFORMITY OF STRESS IN THE GLASS SPECIMEN

The Babinet-Soleil compensator also is used to check on the uniformity of stress across the central one-third of the 30 mm high glass test samples. The need for this method of determining stress uniformity rather than the use of simple crossed Polaroid films became evident in an early comparison of the Zernike three pinhole system with a "Senarmont-with-one-pinhole" technique. Samples under stress which had been adjusted to look quite uniform in their central region when viewed between crossed Polaroid showed a relative retardation,  $\delta$ , ranging from  $41^\circ$  on one side, to  $55^\circ$  at the center, to  $45^\circ$  on the other side when measured with the Senarmont Method. These limits of Polaroid film were corroborated in recent work on mica, which displays sharp steps in thickness and hence  $\delta$ , between crossed Polaroid where the limit of detectability of the steps occurred when  $\delta$  differs by  $5^\circ$  across the step. With continuous variations of  $\delta$ , as in the case of stressed glass, one cannot expect to do as well as  $5^\circ$ .

The following procedure is used to check stress uniformity in the test specimen under pressure. The filtered light from a mercury discharge lamp is aimed so as to illuminate a diffusely transmitting screen backed by a sheet polarizer placed between the collimator lens and the sample cf. Figure 1 (see also Figure 5). The laser light is blocked and the triplet of pinholes is removed. The substitute, diffuse, monochromatic ( $5461\text{\AA}$ ), linearly polarized light source (the plane of polarization is again at  $45^\circ$  to the Z

direction in the glass sample) is viewed through the sample plus the Babinet-Soleil compensator plus the linear polarizer on the compensator. If the glass is not stressed, and the compensator, is set on zero, the field of view can be made dark by crossing the compensator polarizer with that of the diffuse source. When the glass is stressed, the compensator must be adjusted to restore the polarization, whereupon the field through the sample can be made dark again. The more uniformly dark this field is, the more uniform is the stress on the glass block. The eye is rather limited in its ability to judge uniformity under these conditions; it is estimated that the variations in birefringence across the sample can be kept to less than  $10^\circ$  or  $10/360$ , 0.03 wavelength. On the average, the birefringence at the center of the block should not vary from one application of a given load to the next by more than this.

Unfortunately this method of checking uniformity of stress is not sensitive enough to guarantee a repeatability of pathlength change from one application of the load to the next of 0.01 wavelength. More sensitive methods for monitoring the uniformity of stress are available, but they are much more time consuming to use since they are not broad field in nature. It was decided that this limitation on the accuracy of the measurements would be accepted. The accuracy actually achieved was checked by duplicating measurements on some samples on the completed apparatus.

#### 2.4 PRECISION STRAIN FRAME

A photograph of the complete strain frame is shown in Figure 3; a cutaway drawing to clarify the design is shown in Figure 4. In operation, the desired vertical downward force is applied to the specimen by means of a 1 meter long, tapered, lever arm that is counterweighted to avoid the task of determining the loading effect of the arm itself. Weights mounted on a sliding weight hanger allow for selection of the maximum force applied. The outer end of the lever is supported by an adjustable arm rest (N in Fig. 4) when a sample is not being compressed. The fulcrum of the lever is at the center line (A) of a set of ball bearings, the mount for which (B) is supported on two vertical columns (C). The ball bearing mount may be raised or lowered along the support columns by means of a screw which couples the ball bearing mount to a fixed crosspiece (D) which is also clamped to the vertical support columns. In actual practice, this screw is used to lift the ball bearing mount and lever arm enough to allow the test specimen to

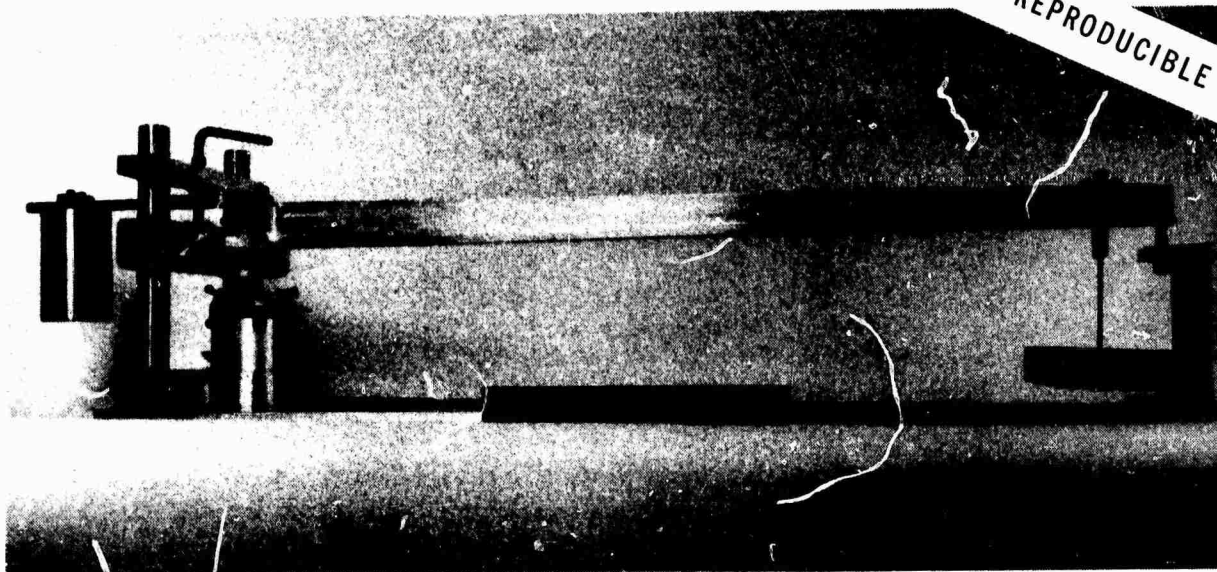


Figure 3. Photograph of the strain frame.

be put in place and then to lower this assembly onto the test specimen until the outer end of the lever arm is lifted free from its arm rest, thus applying the full load to the test specimen.

The lever arm has a hardened steel socket in an anvil (E) on its lower side accurately centered 1.000 inch from the line of centers of the ball-bearings about which the lever arm pivots. The socket accepts a 1/2-inch steel ball (F) that transmits the load to a mating lower anvil (G) whose flat lower surface presses against the upper end of the test specimen (H). A 1/16 inch sheet of neoprene rubber is used to improve the load uniformity between G and H. The sample stands on a platform (J) that is held in a cup-shaped holder (K) with a system of screws for adjustment and locking of position. The mating surfaces between the holder and anvil are ground spherical with a radius of curvature of about 7 cm, a distance calculated to locate the ball (F) and socket of the upper anvils very nearly coincident with their center of curvature when a sample is in place. The sample platform can be moved and clamped in position by three screws (L) acting radially on it; the holder can be rotated in a horizontal plane by a tangent arm and screw (M). These motions are provided so that the glass sample can be adjusted to have its polished surfaces perpendicular to the optic axis of the interferometer prior to any strenuous compression.

The strain frame works satisfactorily to compress the 1x1x3 cm glass samples with loads of 175-250 Kg-wts/cm<sup>2</sup> with little or no sample motion. Some tilt of the sample can be seen when force is applied, but with a little patience the sample can be adjusted to reduce this motion to the recommended level of tolerance.



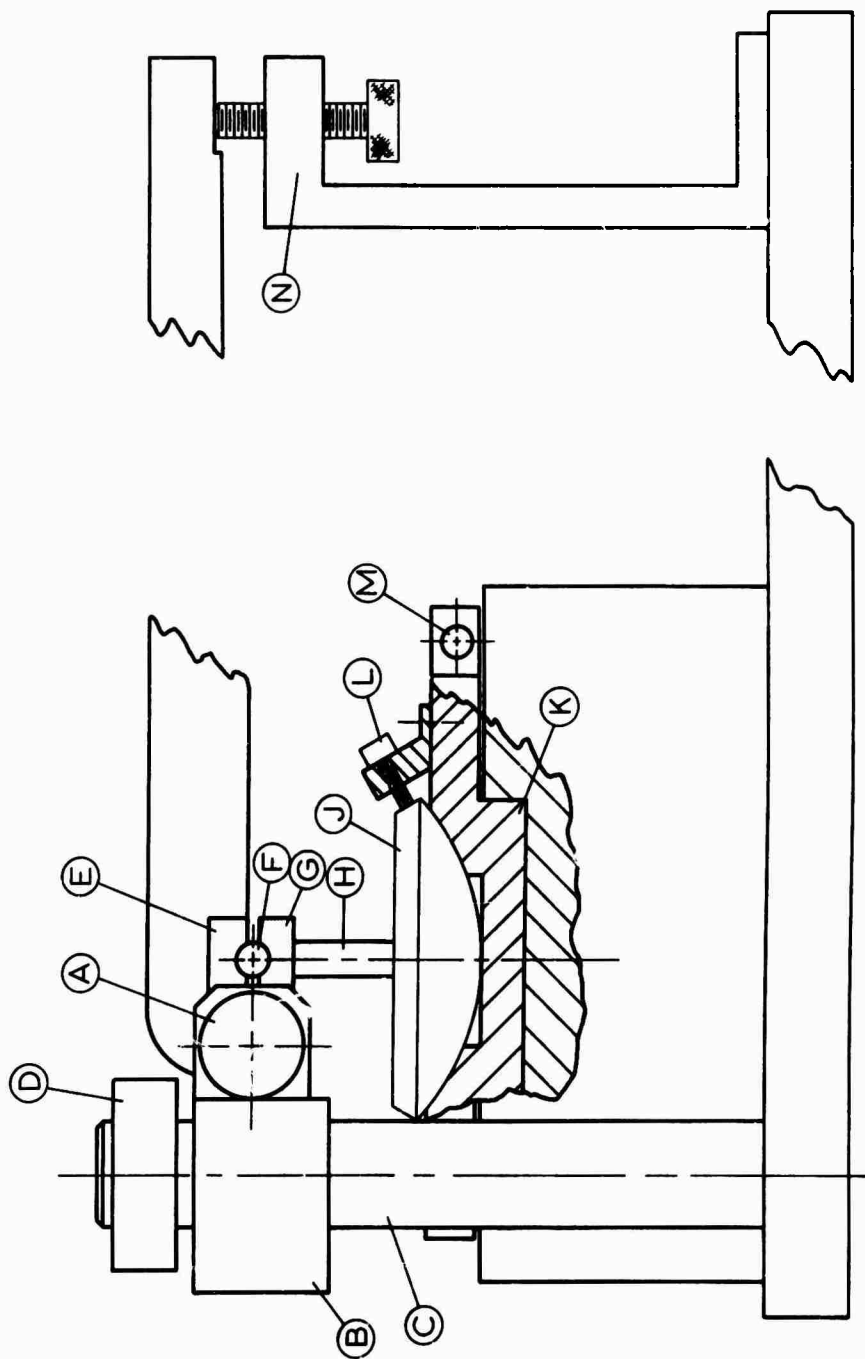


Figure 4.

Figure 4. Schematic drawing of the strainframe.

### 3.0 EXPERIMENTAL PROCEDURE

The components needed for a complete measurement of path-length changes induced by stress in  $1 \times 1 \times 3$  cm glass blocks are shown assembled in Figure 5. The main interferometer is shown lined up parallel to the near edge of the  $4 \times 8$  ft granite vibration isolation table. From upper left to lower right in the photograph they are; the He-Ne laser light source, the collimator-pinhole head assembly, the collimator lens, the strain frame clamped to the table, the telescope lens and the  $100\times$  microscope, with polarizing eyepiece, on its micrometer table. To the right of the collimator-pinhole head assembly are the mercury vapor lamp, 546 Angstrom filter, diffuser and sheet polarizer used to check on uniformity of stress in the glass sample. To the right of the telescope lens in the Babinet-Soleil compensator and polarizing eyepiece used to check on the uniformity of stress in the sample and to measure the birefringence induced by the stress. The wood and sheet plastic framework in the background is placed over the apparatus during the measurements to provide a thermal shield. This framework has panels for access to the various parts of the interferometer.

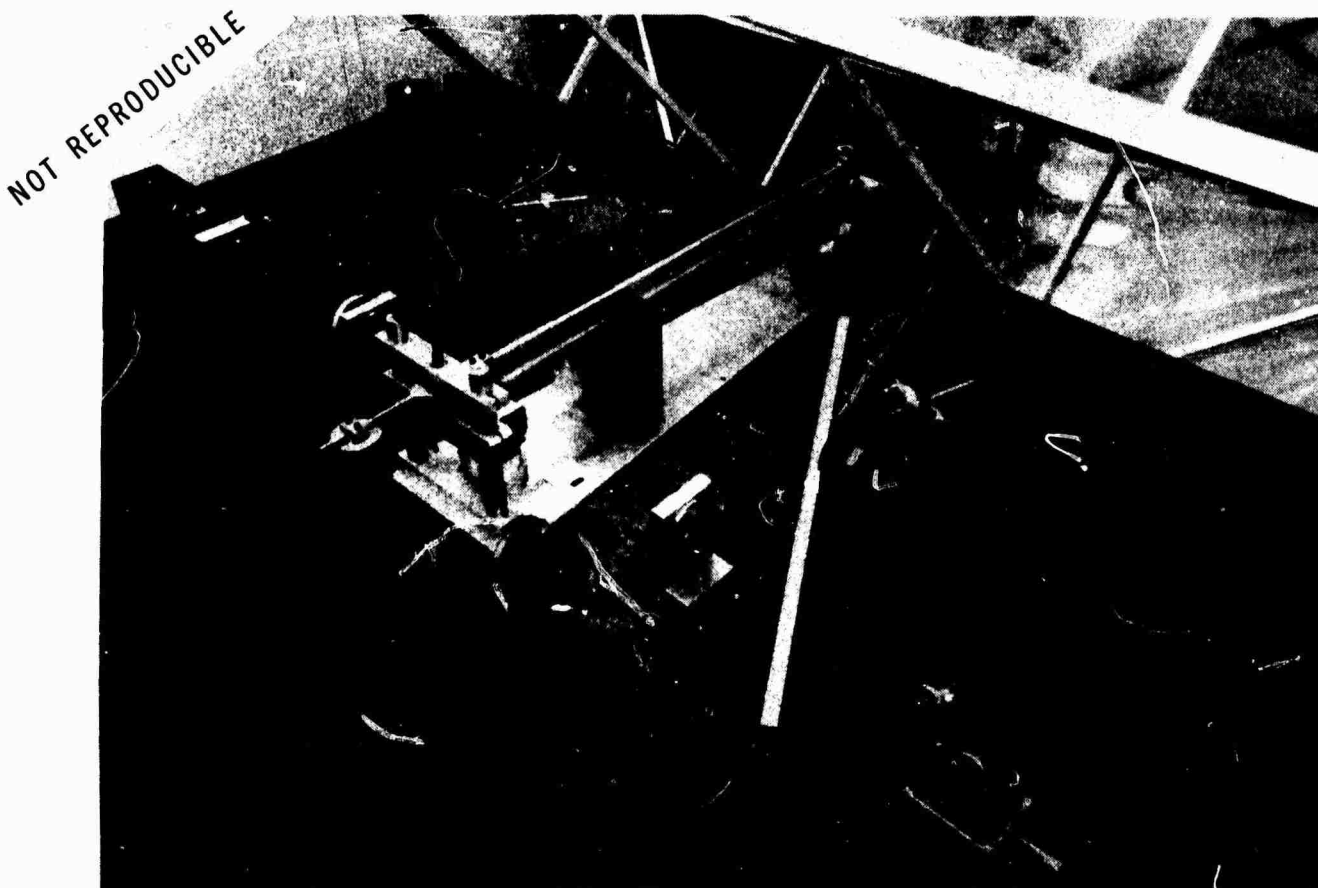


Figure 5. Experimental setup used for complete measurement of stress induced pathlength changes.

After the laser has been turned on and thermal equilibrium has been reached, a measurement is carried out approximately as follows: The glass sample to be examined is positioned in the strain frame and oriented so that its polished faces return images of the illuminating pinhole onto the reticle of the auto-collimator eyepiece. The lever arm of the strain frame is raised and lowered and adjustments of sample orientations are made until the sample can be strained with little or no tilting. Then the uniformity of stress in the strained test specimen is checked using the procedure described in Sect. 2.3. The telescope lens is removed during this check to make room for the compensator, but its base has detents for accurate re-positioning.

When satisfactory stress uniformity has been obtained in the test specimen, the laser light and telescope lens are restored. The sample is stressed moderately, the polished faces are cleaned and the triplet of pinholes is attached to the side of the sample nearest the telescope lens with a minimum of soft wax. An inner thermal shield, the black cardboard box shown displaced to the right of the sample and under the lever arm in Figure 5, is placed around the sample, the access panels on the large thermal shield are closed and observations can begin on the three pinhole interference fringe system now in the field of view of the microscope.

The first step is to determine the no-load position of the fringes and their spacing along the optic axis. Then the motion of these fringes is followed with the microscope on its micrometer table as the sample is slowly stressed until the lever arm and weight on the strain frame rise from the arm rest. When those readings are completed for both directions of polarization, the triplet of pinholes is removed, the compensator is substituted for the telescope lens and a reading is taken of the birefringence induced in the sample by the stress. Then the stress is removed. If the relative pathlength change as measured by the compensator (line 5 of Table I) does not agree with that calculated by taking the difference between the absolute pathlength changes as measured by the three-pinhole interferometer for the X- and Z- polarizations (line 4 of Table I) the measurement is repeated.

A typical set of results for five separate measurements on one sample of glass is listed in Table I.

TABLE I. PATHLENGTH CHANGES  $\Delta\phi$ , INDUCED BY REPEATED STRESSING OF A GLASS SAMPLE. THE CHANGES ARE EXPRESSED IN WAVELENGTHS OF  $6328\text{\AA}$ .

Measurement	#1	#2	#3	#4	#5
$\Delta\phi_Z$	0.703	0.698	0.696	0.709	0.693
$\Delta\phi_X$	1.436	1.408	1.432	1.453	1.455
$\Delta\phi_Z - \Delta\phi_X$	0.733	0.710	0.736	0.744	0.762
B-S.*	0.733	0.712	0.739	0.698	0.737

\*Result from the Babinet-Soleil compensator measurement

As suggested in Sect. 2.3, the variation seen from one measurement to the next is attributed principally to nonuniform strain induced in the sample, i.e. the agreement between lines 3 and 4 is better for a given run than reproducibility between runs. It appears that, as a general figure of merit, the stress-optical coefficients will be determined by this method and apparatus to  $\pm 10\%$  assuming that correct values for Young's Modulus and Poisson's Ratio can be obtained for the glass samples.

## APPENDIX I

### TOLERANCE STUDIES ON THE INTERFEROMETER

#### I.1 EFFECT OF DEFOCUSING THE COLLIMATOR

In setting up the system of Figure 1, it is assumed that with collimators and telescopes of 15 inch focal length one is likely to set point O only within  $\pm 1/4$  inch of the first focal point of the collimator. Similarly, one is likely to set Q only within  $\pm 1/4$  inch of the first focal point of the telescope.

We will now show that, fortunately, a defocusing of the collimator does not introduce error into our measurement of pathlength change.

Suppose first that in Figure 1 the pinhole O falls to the left of the first focal point of the collimator. Then, in the absence of the telescope lens, O would be focused at a point O' at a great distance,  $\ell_o$ , from the plane of the three pinholes as shown in Figure I-1. Let us suppose for simplicity that the system is centered and is highly corrected. Then, the phase at the two outer pinholes will be given by

$$e^{ikC} e^{-ikR} = e^{ikC} e^{-ik\sqrt{a^2 + \ell_o^2}} \quad (1)$$

and the phase at the central pinhole will be given by

$$e^{ikC} e^{-ik\ell_o} e^{i\Delta_a}, \quad (2)$$

where C measures the total pathlength from O to O' and  $\Delta_a$  is the average additional pathlength introduced by the glass sample.

We may now find the solution to the Fresnel problem as done previously (cf. previous report\* Appendix Sections I.4, I.5, and I.6 wherein D corresponds to the present  $\ell_o$ ). For simplicity let the two outer pinholes have the same area A. Our solution for  $F(x,0) = F(x)$  will be that of Eq. (38) of the previous semi-annual report in the above mentioned Appendix wherein

$$\Delta_1 = \Delta_2 = k(C - \sqrt{a^2 + \ell_o^2}) ; \Delta_2 - \Delta_1 = 0; \quad (3)$$

---

\*Neodymium Laser Glass Improvement Program, Technical Summary Report No. 10, Contract Nonr 3835(00) March 1971.

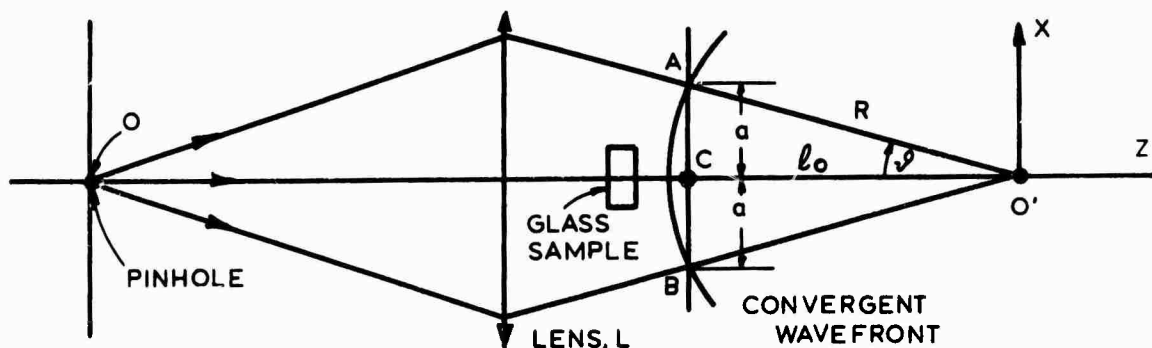


Figure I-1. Illumination of the pinholes A, B and C in convergent light.

and  $\Delta_a$  is replaced by

$$\Delta_a + k(C - l_0) . \quad (4)$$

Maintaining the approximation expressed in Eq. 44 of that Appendix and ignoring the unimportant external factors one obtains, for the case  $A_1 = A_2 = A$ ,

$$F(x) = 2A \cos \left[ \frac{kax}{l_0} \left( 1 - \frac{a^2}{2l_0^2} \right) \right] + T B e^{i\Phi}, \text{ where} \quad (5)$$

$$\Phi \equiv \Delta_a + k \left[ \sqrt{l_0^2 + a^2} - l_0 \right] - \frac{ka^2}{2l_0} \left[ 1 - \frac{a^2}{4l_0^2} \right]. \quad (5a)$$

With the system of Fig. 1 the defocusing of the collimator will be kept small enough so that  $l_0$  will remain great and will be so large relative to  $a$  of Fig. I-1 that we may accept as before the approximation

$$F(x) = 2A \cos \left( \frac{kax}{l_0} \right) + T B e^{i\Phi} ; \quad (6a)$$

$$\Phi = \Delta_a + k \left[ \sqrt{l_0^2 + a^2} - l_0 \right] - \frac{ka^2}{2l_0} . \quad (6b)$$

Solution in the Fresnel plane when the collimator is defocused to produce slightly convergent light.

Let the telescope be inserted so that the three pinholes are at the front focal plane of the telescope and  $O'$  is now brought to focus at  $O''$ , as in Figure I-2, and in accordance with Newton's formula

$$f^2 = -l_o z \text{ or } \frac{1}{l_o} = -\frac{z}{f^2} \quad (7)$$

where  $z$  is the distance measured from the back focal plane of the telescope to  $O''$ . Then from Eqs. 6 and 7

$$\Phi = \Delta_a + k \left[ \sqrt{l_o^2 + a^2} - l_o \right] + \frac{ka^2 z}{2f^2} \quad (8)$$

But

$$\sqrt{l_o^2 + a^2} - l_o = \frac{a^2}{2l_o} \quad (9)$$

$\therefore$

$$\Phi = \Delta_a + \frac{ka^2}{2} \left( \frac{z}{f^2} + \frac{1}{l_o} \right) \quad (10)$$

Now, if  $\Delta_a = 0$ , then  $\Phi$  should equal to zero when  $z$  is the location of the star image formed by the collimator and telescope. From Eq. 10, with  $\Delta_a = 0$  and  $\Phi = 0$ ,

$$-zl_o = f^2 ; \text{ Newton's formula.} \quad (11)$$

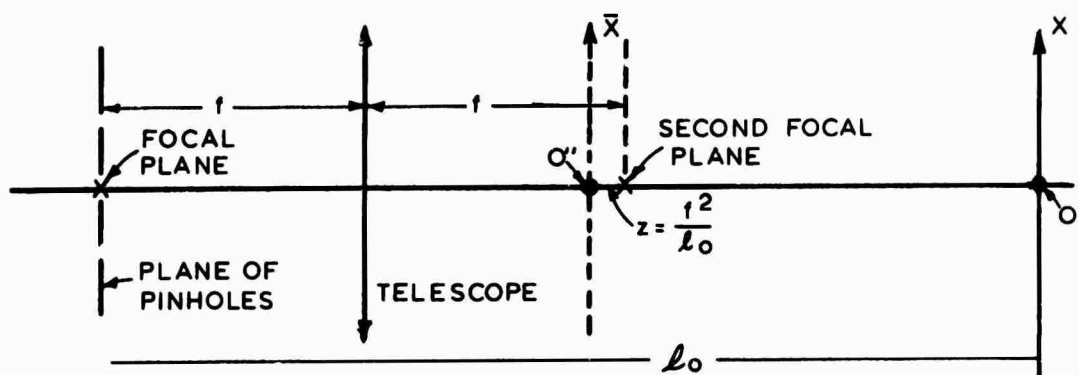


Figure I-2. Location of the star image  $O'$  as formed by collimator alone and of the new image  $O''$  when a telescope is added with its front focal plane coincident with the plane of pinholes.

Therefore when  $\Delta_a = 0$  the plane  $z$  in which  $\Phi = 0$  is the plane of the image of the illuminating pinhole  $O$ .

It follows from Eq. (8) that since  $\sqrt{l_o^2 + a^2} - l_o$  is constant and that if  $z$  is altered so that  $\Phi$  is fixed at  $\mu \frac{\pi}{2}$  where  $\mu$  is a particular odd integer, then

$$(\Delta_a)_2 - (\Delta_a)_1 = \frac{ka^2}{2f^2} (z_1 - z_2) \quad (12)$$

This means that defocusing the collimator so as to obtain slightly convergent light will introduce no error in the measurement of

$(\Delta_a)_2 - (\Delta_a)_1$ . Also, we have seen that  $\Phi$  continues to remain linear in  $z$  provided that the plane of the three pinholes is the front focal plane of the telescope.

Consideration of the case of the slightly diverging beam in which the collimator is defocused so as to image  $O'$ , Figure 1.2 at a great distance  $l_o$  to the left of the three pinholes yields instead of Eq. 10

$$\Phi = \Delta_a + \frac{ka^2}{2} \left( \frac{z}{f^2} - \frac{1}{l_o} \right). \quad (13)$$

The position given by  $zl_o = f^2$  is now that of the final "star image"  $O''$ . The conclusions drawn above hold again.

In conclusion: Defocusing of the collimator in the arrangement of Figure 1 by relatively slight amounts will not alter the accuracy of the measurement of the phase differences

$$(\Delta_a)_2 - (\Delta_a)_1.$$

## 1.2 TOLERANCE ON THE ANGULAR ORIENTATION OF THE INCIDENT ELECTRIC VECTOR IN THE X-Z METHOD

In this method, described in Section 2.2, the incident E-vector is intended to vibrate either along  $Z$  or along  $X$ . We examine here how closely one must set  $E$  along  $Z$  or along  $X$ . In doing so, it suffices to consider the setting with respect to  $Z$  since the same tolerance must apply with respect to the  $X$ -setting.



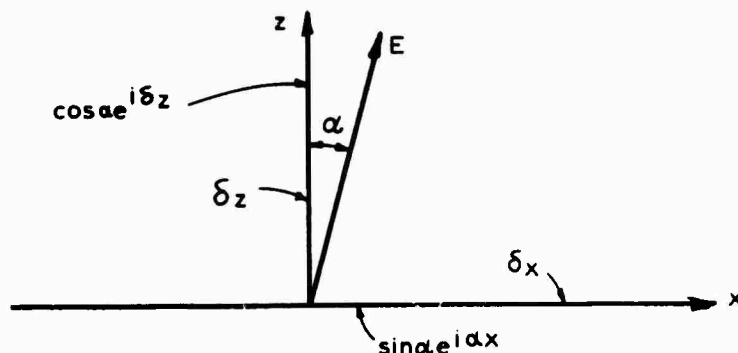


Figure I-3. Convention with respect to establishing a tolerance for the angle  $\alpha$  in the X-Z method.

First, we note that for the two outer, clear pinholes the E-vector remains unchanged in phase, amplitude and direction upon passing through these pinholes. But such is not the case for the light traversing the glass and the central pinhole. Let the strength of the incident E-vector be unity. Then for the E-vector emerging from the central pinhole.

$$\text{Z-component} = \cos \alpha e^{i \delta_z} ;$$

$$\text{X-component} = \sin \alpha e^{i \delta_x} ; \quad (14)$$

where  $\delta_z$  and  $\delta_x$  are the retardations of the strained glass for the Z and X-components, respectively. Since no analyzer is used, the fringes are due to interference of the combined electric vectors that oscillate along the line of vibration of the incident electric vector inclined at angle  $\alpha$  with respect to Z.

Let  $P_r$  denote the projection of the vector described by Eq. 14 upon the direction E. Then

$$P_r = \cos^2 \alpha e^{i \delta_z} + \sin^2 \alpha e^{i \delta_x} = \cos^2 \alpha e^{i \delta_z} [1 + \tan^2 \alpha e^{i(\delta_x - \delta_z)}] \quad (15)$$

As regards the E-vector emerging from the central pinhole, the only part of it that is of any use in forming the interference fringes is that having amplitude and phase given by the complex number  $P_r$ . In case  $\alpha=0$ , the correct value, then simply

$$P_r = e^{i \delta_z}$$

where  $\delta_z$  is the phase that we want to measure. Let

$$\psi \equiv 1 + \tan^2 \alpha e^{i(\delta_x - \delta_z)} \equiv 1 + \tan^2 \alpha e^{i\Delta} ; \quad (16)$$

$$\Delta \equiv \delta_x - \delta_z$$

Then

$$\theta = \arg(\psi) \quad (17)$$

is the error in the phase of the disturbance leaving the central pinhole produced by setting  $\alpha \neq 0$ .

Now

$$\psi = 1 + \tan^2 \alpha \cos \Delta + i \tan^2 \alpha \sin \Delta . \quad (18)$$

$\therefore$

$$\tan \theta = \frac{\tan^2 \alpha \sin \Delta}{1 + \tan^2 \alpha \cos \Delta} , \text{ whence}$$

$$\tan^2 \alpha = \frac{\tan \theta}{\sin \Delta - \cos \Delta \tan \theta} \quad (19)$$

Since both  $\alpha$  and  $\theta$  will be small, we have approximately

$$\alpha = \frac{\sqrt{\theta}}{\sqrt{|\sin \Delta - \theta \cos \Delta|}} \quad (20)$$

The smallest value of  $\alpha$  occurs when  $\Delta$  is near  $\pi/2$ . Hence we take as the tolerance on  $\alpha$

$$|\alpha| \leq \sqrt{\theta} . \quad (21)$$

If the error  $\theta = 1^\circ$  (corresponding to a phase error of  $\lambda/360$ ) is permitted as upper maximum, then

$$|\alpha| \leq \sqrt{\frac{1}{57.3}} \text{ radians} = 7.56^\circ . \quad (22)$$

Correspondingly, the error in the angular setting of the  $\lambda/2$ -plate is  $7.56/2 = 3.78^\circ$ . These are very liberal tolerances. Actually, it is easy to set the  $\lambda/2$  plate within  $\pm 0.2^\circ$  of the correct position.

Experiment showed that the  $\lambda/2$ -plate ought not to be rotated as much as  $1^\circ$  from its correct position but that  $\pm 0.2^\circ$  or even  $\pm 0.3^\circ$  is acceptable. Therefore, no problem arises in setting the  $\lambda/2$ -plate accurately enough in the X-Z method.

### I.3 TOLERANCE ON THE ANGULAR ORIENTATION OF THE ANALYZER IN THE $45^\circ$ METHOD

In this method, the incident E-vector vibrates at  $45^\circ$  with X and Z and the analyzer is set along either X or Z. Consider, Figure I-4, a setting error  $\alpha$  of the analyzer. With the incident polarization P at  $45^\circ$ , emerging from the central pinhole will be

$$\begin{aligned} e^{i\delta_z}/\sqrt{2} \text{ as z-component} & ; \\ e^{i\delta_x}/\sqrt{2} \text{ as x-component} & . \end{aligned} \quad (23)$$

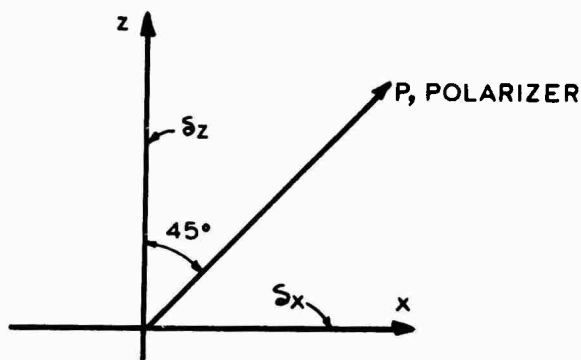


Figure I-4a

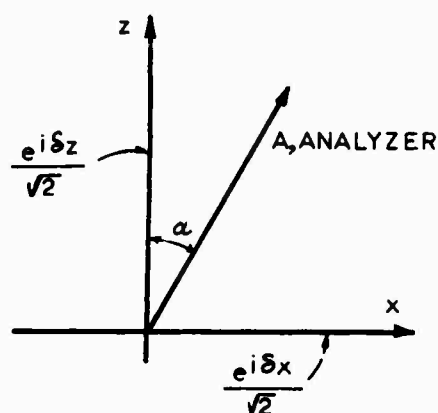


Figure I-4b

Polarized light emerges from the two outer pinholes vibrating along P and undisturbed in amplitude and phase. We have to project all of the disturbances upon the direction of the analyzer in determining the distribution of irradiance in the interference fringes.

The projection of the disturbance (23) upon the analyzer is given by the complex number

$$A = \frac{\cos\alpha}{\sqrt{2}} e^{i\delta_z} + \frac{\sin\alpha}{\sqrt{2}} e^{i\delta_x} = \frac{\cos\alpha}{\sqrt{2}} e^{i\delta_z} [1 + \tan\alpha e^{i\Delta}] , \quad (24)$$

$\Delta \equiv \delta_x - \delta_z$ , the relative retardation.

With the setting of Figure 4b, one is seeking information about  $\delta_z$ . The information will be correct at  $\alpha=0$  where

$$A = e^{i\delta_z} / \sqrt{2} . \quad (25)$$

But with  $\alpha \neq 0$  the disturbance A from the central pinhole will depart in phase from the amount  $\delta_z$  by the error  $\theta$  where

$$\theta = \arg (1 + \tan\alpha e^{i\Delta}) = \arg [1 + \cos\Delta \tan\alpha + i \sin\Delta \tan\alpha] . \quad (26)$$

In the complex Z-plane we have, as in Figure I-5,

$$\tan\theta = \frac{\sin\Delta \tan\alpha}{1 + \cos\Delta \tan\alpha} . \quad (27)$$

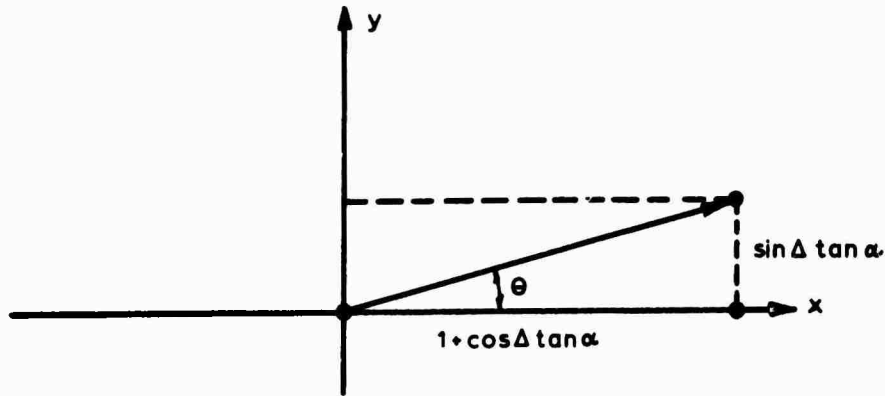


Figure I-5. Representation of the phase error  $\theta$  in the complex Z-plane.

(27)

Then since  $\theta$  and  $\alpha$  will be small

$$\theta = \frac{\alpha \sin \Delta}{1 + \alpha \cos \Delta} \rightarrow \alpha \sin \Delta \quad (28)$$

Whence, approximately,

$$|\alpha| = \left| \frac{\theta}{\sin \Delta} \right|. \quad (29)$$

Since  $|\alpha|$  is smallest when  $|\sin \Delta| = 1$ , we take as our tolerance on  $\alpha$

$$|\alpha| \leq |\theta| \quad (30)$$

Again, we ask that  $\theta$  shall not exceed  $1^\circ$  so that the phase error shall not exceed  $\lambda/360$ . Thus, our tolerance on the setting of the analyzer from its correct position is

$$|\alpha| \leq 1^\circ \quad (31)$$

in the  $45^\circ$ -method.

This tolerance is not difficult to meet.

We conclude that whether one uses the X-Z method or the  $45^\circ$  method the tolerances on the "polarizer" or analyzer settings are large enough so that no difficulty need be expected.

#### I.4 TOLERANCES WITH RESPECT TO IMPERFECT SAMPLES IN THE THREE-PINHOLE, ZERNIKE METHOD

Experiment has indicated that in the presence of striae one must mount the three pinholes so that they ride with the sample. In the following we assume that at least the central pinhole is attached to the sample. In determining the precision with which the samples are to be fabricated the following factors should be considered;

- (A) Effects of non-uniformity of optical path between the polished faces due to the presence of wedge or lack of flatness.
- (B) Non-uniformity of strain in a wedged sample.

- (C) Wedge between the polished faces can cause the diffraction pattern from the central pinhole not to overlap those from the two side holes.
- (D) The relation of wedge-angle to autocollimation.

#### I.5 TOLERANCE ON WEDGE-ANGLES AS RELATED TO THE NEED FOR AUTOCOLLIMATION

We refer here to wedge between the two polished faces. The tolerance on wedge-angle becomes so liberal that one can ignore it provided that upon autocollimation one takes the trouble to distinguish carefully between the two images produced by reflection from the two polished faces. Owing to the presence of striae, the image reflected from the second surface is usually blurred.

The penalty for paying no attention to this matter will be to keep the wedge-angle down to about 1 minute of arc in order to control the tilt of the sample as the pressure is altered. We assume that proper care will be taken during autocollimation so that no tolerance beyond the normal care taken in the optical shop need be assigned relative to the matter of controlling the tilt of the sample.

#### I.6 TOLERANCE ON WEDGE ANGLES AS REGARDS OBTAINING RELIABLE MEASUREMENT OF THE AVERAGE OPTICAL PATH

Fortunately, this aspect of the measurement does not require the assignment of tolerance of wedge-angles beyond routine practice in the optical shop.

From Eqs. (5.4) and (5.5) in Section 5 of the previous semiannual report we have to consider the integral

$$I = \underbrace{\iint_{\text{over central pinhole}} P_o(\zeta, \eta) d\zeta d\eta}_{\text{over central pinhole}} = T e^{i\Delta_a} \underbrace{\iint_{\text{over central pinhole}} e^{i[\Delta(\zeta, \eta) - \Delta_a]} d\zeta d\eta}_{\text{over central pinhole}} \quad (32)$$

where  $\Delta_a$  is the averaged optical path over the pinhole. Let

$$\psi \equiv \iint_{\text{over central pinhole}} e^{i[\Delta(\zeta, \eta) - \Delta_a]} d\zeta d\eta \quad (33)$$

We have to keep firmly in mind that in measuring the stress-optical coefficients we measure  $\arg(I)$  at two different pressures and then subtract these arguments (phases) from each other with the aim of measuring in this way

$$\Delta = (\Delta_a)_{\text{at } P=P_2} - (\Delta_a)_{\text{at } P=P_1} \quad (34)$$

For this to be true our experimental conditions must be such that

$$\text{Arg}(\psi) = \text{constant, independent of pressure.} \quad (35)$$

It is not necessary that  $\arg(\psi) = 0$ .

Assume for simplicity that the incident wavefront is normal to the optic axis. The effect of a wedged sample is to incline this wavefront into oblique incidence upon the central pinhole. Without loss of generality we may regard  $\zeta, \eta$  to be oriented so that correspondingly  $\Delta(\zeta, \eta) = \Delta(\zeta) = \Delta_a + K\zeta$

(36)

where  $K = \frac{2\pi}{\lambda} (n-1) A$  ;  $A$  = angle of the wedge.

(37)

Then from Eqs. (33) and (36)

$$\psi = \iint_{\text{over central pinhole}} e^{iK\zeta} d\zeta d\eta \quad (38)$$

Let the central pinhole be circular with area  $B$ . Then, introducing polar coordinates

$$\psi = \int_0^{\sqrt{\frac{B}{\pi}}} \int_0^{2\pi} e^{iK\rho\cos\theta} \rho d\rho d\theta = 2\pi \int_0^{\sqrt{\frac{B}{\pi}}} J_0(K\rho) \rho d\rho \quad (39)$$

$$\psi = \pi \frac{B}{\pi} 2 \frac{J_1(K\sqrt{\frac{B}{\pi}})}{K\sqrt{\frac{B}{\pi}}} \quad (40)$$

Then since  $\frac{B}{\pi} = R_c^2$  = radius of the central pinhole,

$$\psi = 2B \frac{J_1(KR_c)}{K R_c} ; \quad \underline{\text{real}} ; \quad (41)$$

$R_c$  = radius of central pinhole;  $B = \pi R_c^2$  ;

$K = \frac{2\pi}{\lambda} (n-1) A$  ;  $A$  = angle of the wedge.

Hence if the polished faces form a simple wedge,

$$\arg(\psi) = 0 \text{ for all pressures} \quad (42)$$

irrespective of the wedge angle. Hence we do not have to assign a tolerance on the wedge angle from the considerations of this section. This conclusion was unexpected.

#### I.7 TOLERANCE ON SURFACE FLATNESS AS REGARDS OBTAINING RELIABLE MEASUREMENT OF THE AVERAGE OPTICAL PATH

It will not be possible to examine here all possible variations from surface flatness; but the special case studied here suggests strongly that as regards measuring  $[(\Delta_a)_{P_2} - (\Delta_a)_{P_1}]$  properly from the restricted viewpoint of this section, no tolerances need be assigned to surface flatness beyond the quality which is routine in our optical shop.

We can expect that for radially symmetric surface deviations from flatness

$$\Delta(\zeta, \eta) = \Delta_a + \sigma(\zeta^2 + \eta^2) \quad (43)$$

when the central pinhole is placed over the center of the irregularity. Then from Eqs. (32) and (33)

$$\psi = \iint_{\text{over central pinhole}} e^{i\sigma(\zeta^2 + \eta^2)} d\zeta d\eta. \quad (44)$$

Let the central pinhole be circular with radius  $R_c$  and area  $B$ . Upon converting to polar coordinates, we obtain

$$\psi = 2\pi \int_0^{\sqrt{\frac{B}{\pi}}} e^{i\sigma\rho^2} \rho d\rho = 2\pi \int_0^{R_c} e^{i\sigma\rho^2} \rho d\rho ;$$

$$\psi = -\frac{i\pi}{\sigma} e^{iz} \Big|_0^{\sigma R_c^2} = \frac{i\pi}{\sigma} [1 - e^{i\sigma R_c^2}] . \quad (45)$$

As  $\sigma R_c^2 \rightarrow 0$ ,

$$\psi \rightarrow \frac{i\pi}{\sigma} (-i) \sigma R_c^2 = B ; I \rightarrow T B e^{i\Delta_a} . \quad (45a)$$



We observe from (45) that whereas  $\arg(\psi)$  is not in general equal to zero (the exception occurs when  $\sigma R_C^2 \rightarrow 0$ ) it is in a given set-up a constant independent of pressure. Hence this type of surface error (and we can suspect all others, need not be assigned tolerances beyond the quality which is routine in our optical shop. This is, of course, fortunate.

# 1.8 TOLERANCE IMPOSED ON THE ANGLE OF THE WEDGE IN ORDER THAT THE DIFFRACTION PATTERNS SHALL OVERLAP PROPERLY

It turns out that a tolerance on the angle of wedge between the two polished surfaces needs to be imposed in order that the light diffracted from the three pinholes shall overlap properly in the plane of observation. In calculating this tolerance, we need consider only the far Fresnel region as in Section 4 of the previous semiannual report where it is estimated that said Fresnel plane is in excess of 50 meters, in our proposed optics, from the plane of the pinholes in the absence of the telescope.

First, for pinholes of about 0.34 mm diameter the radius  $r_a$  of the "Airy disk" in the observation plane is given approximately by

$$r_a = \frac{0.61 \lambda}{N.A.} = \frac{0.61 \times 0.6328 \times 10^{-3}}{\frac{0.34}{2 \times 5 \times 10^4}} = 114 \text{ mm} \quad (46)$$

Secondly, the spacing of the fringes produced by light from the two outer pinholes of separation  $2a = 14 \text{ mm}$  is given by

$$\frac{x}{R} = \frac{\lambda}{2a} \quad \text{whence} \quad x = \text{spacing} = \frac{0.6328 \times 50}{14} = 2.3 \text{ mm} \quad (47)$$

This is in the far Fresnel plane for which  $R = 50 \text{ m}$ . About 100 fringes would then be seen across Airy disks that overlap completely. If the three pinholes are separated by 7 mm and have the same diameter, as is our case, we obtain in the observation plane corresponding to  $R = 50 \text{ m}$ , under idealized conditions three overlapping and interfering diffraction disks each about 114 mm in diameter with their centers displaced each by 7 mm. The effect of placing a glass wedge over the central pinhole is to displace the Airy disk produced by the central pinhole. It is recommended

that this Airy disk be displaced no more but that the irradiance produced by it at the midpoint between the centers of the two outer Airy disks drops to only 90% of its value at the diffraction head.

Approximately,  $\left[2 \frac{J_1(Z)}{Z}\right]^2 = 0.90$  for  $Z = 0.64$ . This means that the central diffraction disk should not be displaced in excess of

$$\frac{0.64}{3.83} \times 114 = 20 \text{ mm.} \quad (48)$$

The angle  $\alpha$  through which light from the central pinhole can be deviated should, then, not exceed

$$\alpha = \frac{20}{5 \times 10^4} = 0.0004 \text{ radians.} \quad (49)$$

The angle of the glass wedge is about twice this value of  $\alpha$  since  $n$  is roughly 1.5. Thus the angle  $A$  of the glass wedge should obey the tolerance

$$A \leq 0.0008 \text{ radians} = 2.7 \text{ minutes.} \quad (50)$$

We regard this as a conservative estimate - meaning that slightly larger angles may prove to be tolerable.

We note that experimentally all of our glass samples that were tested gave good, straight fringes.

#### 1.9 ADDITIONAL COMMENTS ON THE TOLERANCE ON TILT OF THE SAMPLE

A tolerance on tilt of the sample as discussed in 1.8 of the previous semiannual report can be estimated from Eq. (68) of that report as follows:

$$\frac{\delta}{\lambda} = \frac{n-1}{n} \frac{L}{\lambda} \frac{\theta^2}{2} ; \quad \frac{d(\delta/\lambda)}{d\theta} = \frac{n-1}{n} \frac{L}{\lambda} \theta ; \quad (51)$$

where  $\theta$  is the angle between the axis of the instrument (more particularly, the rays of the incident light beam) and the normal to the plate being tilted.

The autocollimator device we have designed for the final apparatus is estimated to permit us to monitor  $\theta$  to at least 10 sec. of arc. Adjusting screws will permit the readjustment of the sample to at least 0.0001 radians or about 21 sec. If we call for a change in  $(\delta/\lambda)$  after readjustment of not more than 0.001, then the angle of tilt  $\theta$  must not exceed

$$\theta = \frac{n}{n-1} \frac{\lambda}{L} \frac{d(\frac{\delta}{\lambda})}{d\theta} = \frac{1.5}{0.5} \frac{0.6328 \times 10^{-3}}{10} \frac{0.001}{0.0001} \text{ so that}$$

as a tolerance on  $\theta$

$$\theta \leq 0.00190 \text{ radians} \approx 7 \text{ minutes.} \quad (52)$$

This tolerance should be easy to maintain mechanically. With the proposed collimating system one will not be able to measure the 7 minutes; but setting within these 7 minutes should be easy.